Report

Current Biology

Pigeons make slow, divergent eye movements during flight and large, convergent eye movements when landing

Graphical abstract

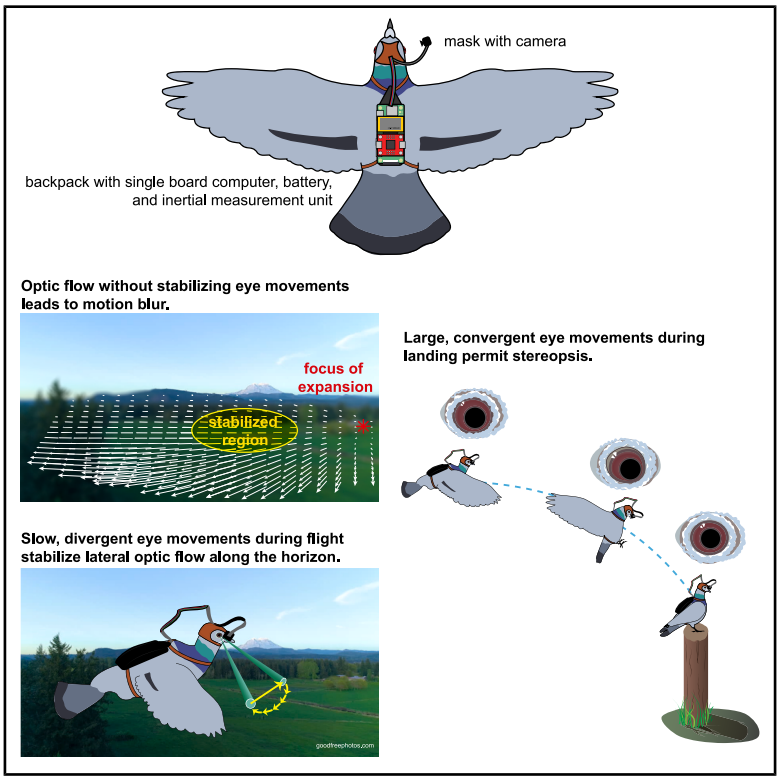

Authors

Anthony B. Lapsansky, Douglas R. Wylie, Douglas L. Altshuler

Correspondence

tony.lapsansky@gmail.com (A.B.L.), dwylie@ualberta.ca (D.R.W.), doug.altshuler@ubc.ca (D.L.A.)

In brief

Contrary to prior assumptions, Lapsansky et al. use onboard cameras to show that pigeons make substantial eye movements during flight, including slow drifting movements that stabilize optic flow and large, convergent movements during landing that permit stereoscopic depth perception.

Highlights

- We tracked eye position and optic flow in pigeons with an onboard camera
- Flying pigeons made slow, divergent eye movements
- Eye movements matched the speed and direction of optic flow
- Landing pigeons made large, convergent eye movements that permit stereopsis

Lapsansky et al., 2026, Current Biology *36*, 1–10
August 3, 2026
https://doi.org/10.1016/j.cub.2026.06.015

CellPress

Current Biology

CellPress

Report

Pigeons make slow, divergent eye movements during flight and large, convergent eye movements when landing

Anthony B. Lapsansky,[1,3,*] Douglas R. Wylie,[2,*] and Douglas L. Altshuler[3,4,5,*]
[1]Salish Sea Research Center, Northwest Indian College, Bellingham, WA 98226, USA
[2]Department of Biological Sciences, University of Alberta, Edmonton, AB, T6G 2R3, Canada
[3]Department of Zoology, University of British Columbia, Vancouver, BC, V6T 1Z4, Canada
[4]Senior author
[5]Lead contact
*Correspondence: tony.lapsansky@gmail.com (A.B.L.), dwylie@ualberta.ca (D.R.W.), doug.altshuler@ubc.ca (D.L.A.)
https://doi.org/10.1016/j.cub.2026.06.015

SUMMARY

As animals move through the world, images of surfaces and edges in the environment move across the retina, a visual signal known as optic flow.[1] Optic flow is beneficial for several processes, perhaps most notably navigation,[2] but it poses a conundrum. When faced with optic flow, the optomotor body, head, and eye movements reflexively minimize optic flow to maintain a stable retinal image.[3] This retinal image stabilization is essential for normal visual function.[4,5] How then can an animal move through the world yet maintain a stable retinal image? Birds are known for their remarkable head stability and also exhibit a variety of eye movements, including rapid and stabilizing vestibular and optokinetic eye movements.[6,7] However, it remains unknown if they move their eyes during flight.[8,9] We developed an onboard camera system to separately track eye movements and record optic flow from homing pigeons (*Columba livia domestica*; hereafter pigeons) released several kilometers from their home loft. During flight, the eyes of pigeons exhibit slow, temporal eye movements consistent with a divergent optokinetic response. These eye movements matched optic flow along the horizon generated by forward flight. Head-restrained pigeons exhibited binocular divergent eye movements in response to computer-generated visual stimuli simulating self-translation. These results are consistent with pigeons stabilizing the horizon in the lateral visual fields during flight. By contrast, during landing, pigeons exhibited large, convergent binocular eye movements directed toward the perch, allowing for stereopsis. In summary, both optokinetic and convergent eye movements appear important for avian flight control.

RESULTS

Pigeons make slow naso-temporal eye movements during flight

To determine whether pigeons make eye movements during flight, we developed a miniature, battery-powered eye-tracking system (Figure 1A). A single-board computer, battery, and inertial measurement unit (IMU) were carried as a backpack (27 g), while the small camera (90 Hz; <1 g) was oriented perpendicular to the head and level with the eye via a custom-fitted mask (Figure 1B; 3 g). Based on the dimensions of the camera and distance to the eye, the eye-tracking system obscured a strip 13°–20° in width across the upper half of the monocular visual field. We used DeepLabCut[10] to track the pupil and features around the margins of the eye. Eye positions were translated into their horizontal and vertical components in an ego-centered reference frame based on the orientation of the lower margin of the eye ring, which aligns closely with the global horizon across behaviors,[11] confirmed by recording a portion of flights with a wide-angle lens (Figure 1C). To reduce the impact of camera vibration caused by locomotion, the pupil position was determined relative to stable features on the head (Figure 1D; Video S1). After categorizing behavior based on data from the onboard IMU (Figure 1E), we translated relative pupil positions to eye-in-head angle (Figure 1F) via an individual-specific calibration procedure (Figure S1; see STAR Methods).

We collected data from 5 individuals and 16 flights, totaling 27 min of flight, 29 min of standing, and 9 min of walking (Video S1). Eye movements were generally limited to ±5 deg of the neutral position, consistent with previous work in pigeons.[13] Free-moving pigeons blinked frequently while flying (2.2 ± 0.4 Hz), walking (2.1 ± 0.2 Hz), and standing (1.4 ± 0.3 Hz), interrupting eye tracking, shown as gaps in the eye position data stream (Figure 1G; Video S1). As a form of low-pass filtering robust to these gaps, we used least-squares linear fits to extract the velocity of the eye (slope) and changes to eye-in-head position occurring during blinks (offset between successive fits). As rapid eye movements represent a break in stable tracking, we detected and removed saccades (Figures 1H and 1I), essentially grouping blinks and saccades together. Saccades were rare

Please cite this article in press as: Lapsansky et al., Pigeons make slow, divergent eye movements during flight and large, convergent eye movements when landing, Current Biology (2026), https://doi.org/10.1016/j.cub.2026.06.015

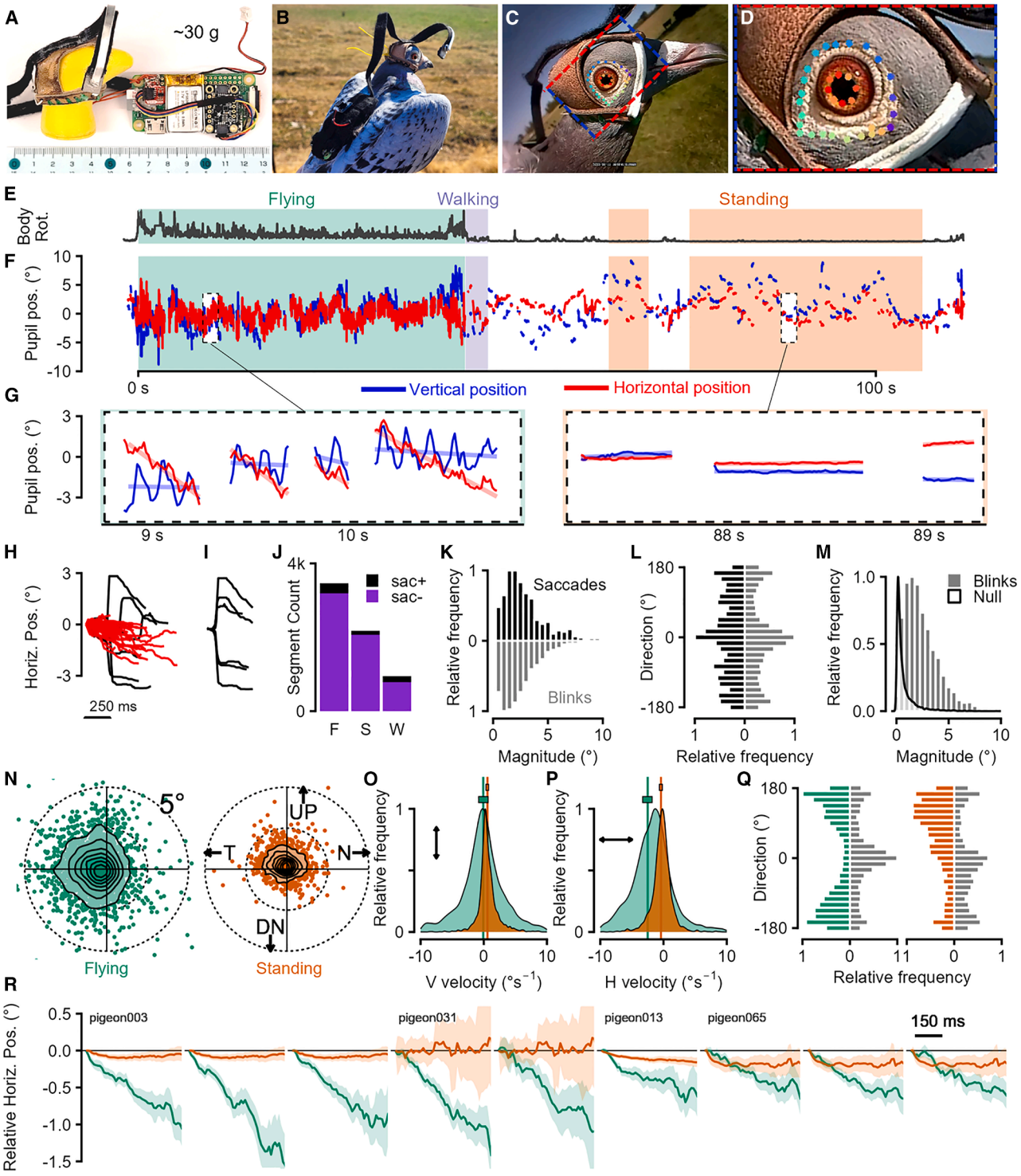

Figure 1. Pigeons make slow temporal eye movements during flight

(A and B) Equipment for recording eye movements, shown isolated and mounted on a pigeon.

(C) DeepLabCut was used to track the pupil and outer margin of the eye ring, an unfeathered region surrounding the eye,[12] shown overlayed on an example frame.

(D) The orientation of the lower eye ring was used to separate horizontal (red) and vertical (blue) directions in head-centered coordinates.

(E) An onboard IMU was used to categorize behavior.

(F) Eye position during a short trial. Positive is dorsal/nasal, and negative is ventral/temporal, for vertical/horizontal eye position.

(G) Zoomed regions for flight (left) and standing (right). Gaps represent blinks. Eye velocity and displacement for each interblink interval were determined by linear regression (transparent lines).

(legend continued on next page)

Please cite this article in press as: Lapsansky et al., Pigeons make slow, divergent eye movements during flight and large, convergent eye movements when landing, Current Biology (2026), https://doi.org/10.1016/j.cub.2026.06.015

(Figure 1J) but resulted in similar changes to eye position as blink-associated eye movements (Figures 1K and 1L), suggesting a shared function.

To test whether rapid eye movements were associated with blinking, we performed a permutation test with trial and behavior included as nested factors. We compared the change in position during blinks to a distribution of null changes selected from the same trial and behavior. Each null value was generated by sampling eye position changes across an equal number of randomly selected time windows (Figure 1M), and each matched in duration to a blink interval (see STAR Methods for additional details on statistical tests). No permutations resulted in changes greater than the actual data ($p < 0.001$), indicating that blinks are associated with rapid eye movements, as in mammals.[14] Blinking may therefore function as a simple form of saccadic suppression.[15] An added benefit of blinking during rapid eye movements is that this coordination minimizes interruptions to visual perception.

We next asked whether birds exhibit slow eye movements during flight. It is widely assumed that animals with laterally placed eyes, like pigeons, should lock their eyes in place between rapid eye movements to simplify self-motion perception.[7,16] Self-motion produces optic flow, which can be used to infer elevation,[17] heading,[18,19] avoid collisions,[20] and regulate speed.[21] Slow eye movements during flight would corrupt the optic flow signal reaching the brain and thereby complicate self-motion perception and flight control. Nevertheless, restrained birds,[22] *Drosophila*,[23] and humans[24] exhibit slow eye movements in response to optic flow—so-called optokinetic eye movements. Compensating for optic flow in this way could help to preserve spatial detail by reducing motion blur[25,26] and facilitate the detection of moving objects.[27] We recently demonstrated that head-restrained hummingbirds compensate for optic flow simulating flight with divergent optokinetic eye movements.[9]

If pigeons compensate for optic flow through optokinetic eye movements, the eye should frequently drift in the temporal direction during flight, as forward flight generates primarily nasal-to-temporal optic flow. In notable contrast, eye movements generated by the vestibulo-ocular reflex (i.e., head rotations[28]) would have a roughly even direction distribution of both nasal and temporal and perhaps also dorsal and ventral movements.[29] As well, pigeons are known to fly with a remarkably stable head between head saccades.[8] Walking pigeons bob their heads,[30] and our equipment did not directly record head movement. Thus, we focus on comparing oculomotor behavior between flight and standing, as the head is held stable between head saccades during both of these behaviors.[8]

A temporal bias was apparent in both eye displacements (Figure 1N) and velocities (Figures 1O and 1P) during flight but not standing. To test whether these observed differences were significant, we performed a randomization test by reshuffling velocities between behaviors from the same individual and comparing the true difference in means between behaviors to the distribution of null differences. Horizontal velocities differed significantly between flight and standing ($p < 0.001$), whereas vertical velocities did not ($p = 0.076$).

The temporal bias during flight requires a mechanism to reset eye position, as the eye would otherwise quickly hit the limit of its range of motion. This occurs during blinks and their associated rapid eye movements, as indicated by the inverse relationship between the direction of eye movements between blinks and those occurring during blinks (Figure 1Q, left). Because an inverse relationship could be seen as an artifact of our method of extracting eye movements, we performed a similar comparison for standing (Figure 1Q, right), but in this case, we found no relationship.

To explore these slow eye movements further, we plotted the eye position across all interblink and intersaccadic intervals, aligned to their starting position. We elected to perform this analysis for the 9 most direct flights ($n = 4$ birds) from the distant release site to the home loft (Figure 1R). Given their durations and distance covered—163 ± 13 s for a displacement of 2.05 km—these flights should have minimal self-rotation relative to self-translation. We compared these data to standing data from the same birds. There was a significant temporal drift during all 9 flights (non-overlapping 95% CI_{boot}). For one bird, the eye also drifted temporally while standing, though the magnitude of this drift was less than occurred during flight for the same animal. Together, these data indicate that flying pigeons consistently make slow temporal eye movements, suggesting that birds exhibit an optokinetic response during flight.

Slow temporal eye movements match optic flow generated by flight

We next asked if the slow temporal eye movements we recorded in free flight matched the optic flow produced by flight. We modified our eye-tracking system with an outward-facing camera oriented along the optical axis of the eye (60° lateral from straight ahead[31]) to record a bird's-eye view during flights from the same release location (Figure 2A; Video S2). This camera captured data for approximately 120° horizontally and 100°

(H and I) Interblink intervals containing saccades (black) were separated from those without (red) using a velocity threshold and split at the saccade into two distinct interblink intervals.
(J) Saccades were rare.
(K and L) Eye movements during blinks and saccades, measured as the offset between successive interblink intervals, had similar magnitudes and directions, suggesting a shared function.
(M) Blink-associated eye movements were larger than expected for their durations, relative to null distributions generated from randomly sampled intervals from the same trial. Representative null shown in white.
(N–Q) (N) Changes to eye position during interblink intervals were biased toward the temporal direction in flight but not standing—also evident in eye velocities (O) and (P)—and (Q) opposite to those occurring during blinks/saccades. Vertical lines in (O) and (P) are medians, and rectangles are 95% CI_{boot}, for each distribution.
(R) Eye position, when aligned to their horizontal onset, showed consistent temporal drift across 9 direct flights, suggesting optic flow compensation (solid line, mean; shaded area, 95% CI_{boot}).
See also Figure S1 and Video S1.

Please cite this article in press as: Lapsansky et al., Pigeons make slow, divergent eye movements during flight and large, convergent eye movements when landing, Current Biology (2026), https://doi.org/10.1016/j.cub.2026.06.015

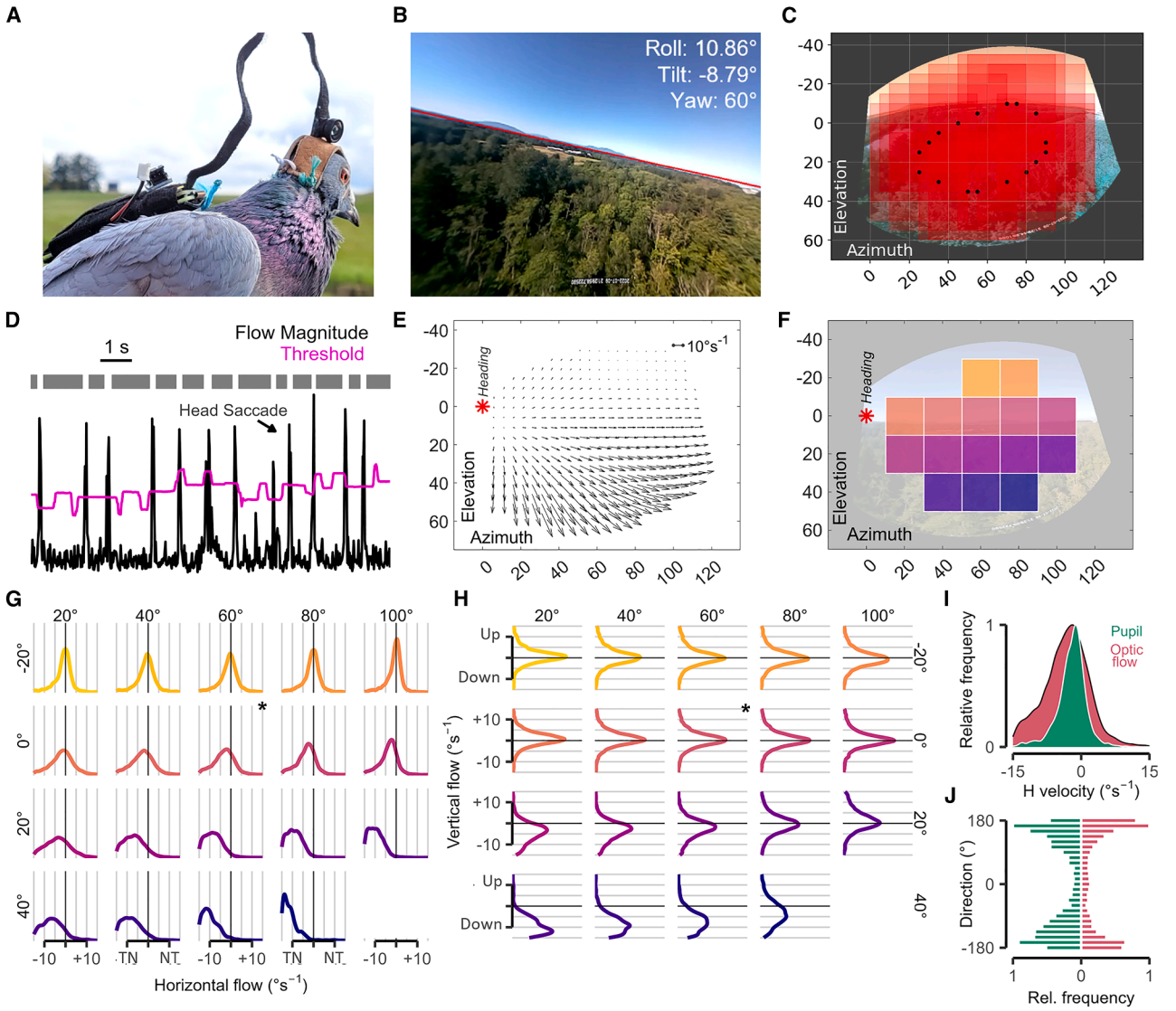

Figure 2. Optic flow along the horizon matches slow eye movements during flight

(A) Equipment for measuring optic flow in flight.

(B) Example camera frame, transformed to rectilinear perspective, with automated horizon detection (red line).

(C) The median position of the horizon from 100 pseudo-random frames was used to reproject each video into a common set of bird-centered coordinates, shown in (C). Optic flow was computed by tiling each video with square patches (red and black dots show patch centers) and computing the median flow across any overlapping regions. Horizontal flow values were adjusted based on latitude to account for the distortion created by the equirectangular projection.

(D) Optic flow was segmented by excluding head saccades, as indicated by flow greater than 2 SD above a 1s moving mean (magenta). Remaining segments (gray rectangles) represent windows of optic flow analogous to interblink intervals for eye movements.

(E) Median flow vectors after removing head saccades, spaced at 5° intervals, for the flight shown in (B)–(D).

(F) To summarize the optic flow across trials, we calculated spatial medians across a consistent set of 20°-by-20° ROIs. ROIs near and beyond the edge of each video were dropped.

(G and H) Across all 34 flights, horizontal (G) and vertical (H) optic flow during flight by location in the visual field.

(I and J) Velocities (I) and directions (J) of the eye mirror but do not exceed those of optic flow along the horizon during flight, which is consistent with ocular compensation for optic flow. Optic flow data in (I) and (J) are compared with the starred panel in (G) and (H).

See also Videos S2 and S3.

vertically, occupying a large portion of the pigeon's monocular visual field. We aligned each video (34 flights, 11 birds) to the same ego-centered reference frame as our eye movement data by transforming the video to a rectilinear perspective, detecting the horizon across 100 pseudo-random frames (Figure 2B), and then reprojecting the video to an equirectangular projection based on this fixed offset (Figure 2C). We then calculated optic flow for each degree of visual angle by tiling the video with overlapping patches (to fill the non-rectangular region of video data), correcting the horizontal components for equirectangular distortion in proportion to the cosine of latitude[32] (Video S3; see STAR Methods).

Please cite this article in press as: Lapsansky et al., Pigeons make slow, divergent eye movements during flight and large, convergent eye movements when landing, Current Biology (2026), https://doi.org/10.1016/j.cub.2026.06.015

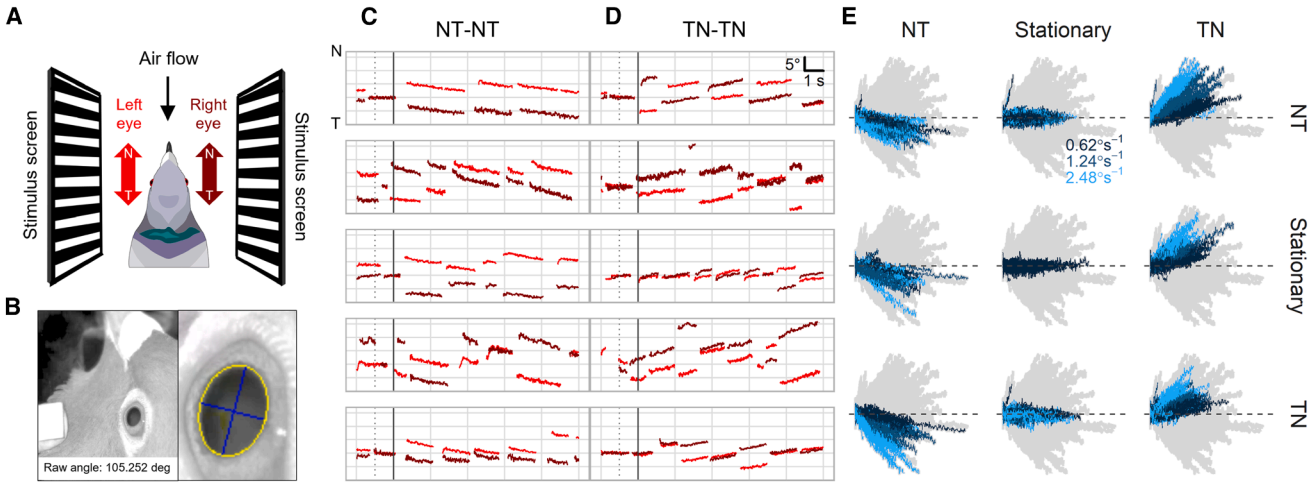

Figure 3. Restrained pigeons compensate for simulated optic flow with slow eye movements

(A) System for recording binocular optokinetic responses in head-restrained pigeons (N, nasal; T, temporal). A fan was placed before the bird to generate feather vibration. Stimulus spatial frequency: 0.8 cycles per degree; square wave; velocities of 0° s^{-1}, 0.62° s^{-1}, 1.24° s^{-1}, and 2.48° s^{-1}.

(B) Example frame (left) from a leveled camera used for head-fixed recording. Ocular orientation was determined by fitting an ellipse to the pupil (right).

(C and D) Representative trials from 5 individuals (rows) demonstrate the capacity for divergent and convergent optokinetic in response to simulated forward (NT-NT) and backward (TN-TN) translation, respectively. Horizontal grid with 5° spacing; vertical grid with 2 s spacing; stimulus velocity 1.24° s^{-1}.

(E) Optokinetic responses of the left eye for combinations of stimuli shown to the left (columns) and right (rows) eyes. Colors indicate stimulus speeds, shown overlayed on all recorded data (gray). Pigeons consistently exhibited compensatory responses for motion simulating translation in both NT-NT and TN-TN stimulus combinations, validating the capacity for this behavior in flight.

As mentioned previously, behaving birds interrupt periods of head stabilization with rapid reorientations of the head, known as head saccades, during which optic flow is disrupted and birds frequently blink.[8,33] We removed optic flow generated by head saccades by employing a moving threshold (Figure 2D), leaving only optic flow produced by translation of the stable head (Figure 2E) separated into discrete chunks analogous to interblink intervals. To summarize the optic flow across trials, we calculated the median flow across a consistent set of 20° × 20° regions of interest (ROIs) (Figure 2F).

Horizontal flow velocities varied consistently across the visual field, with the distribution of velocities centered near zero in the dorsal nasal region of the visual field and becoming increasingly negative in both ventral and temporal directions (Figure 2G). Vertical flow velocities, by contrast, were centered near zero in the dorsal temporal region of the visual field and became increasingly negative in both ventral and nasal directions (Figure 2H). This is consistent with Gibson's original representation of optic flow during flight with a primarily cloudless sky.[1]

Velocities occurring along the horizon were relatively constant and closely matched both the magnitudes (Figure 2I) and directions (Figure 2J) of eye movements during flight. This suggests that flying pigeons make slow temporal eye movements to stabilize optic flow occurring near the lateral horizon.

Pigeons execute slow, divergent eye movements to visual motion simulating flight

Self-translation generates optic flow on both sides of the animal, but our camera equipment was only able to record data for one eye due to weight limitations. To test whether pigeons will execute slow temporal eye movements in both eyes simultaneously—i.e., divergent optokinetic eye movements—we studied head-restrained pigeons[34] (n = 5), permitting simultaneous recording from both eyes and eliminating vestibular input. We positioned pigeons in a flying posture and presented visual stimuli on screens positioned on either side of the animal (Figure 3A). Eye position was extracted from dorsal-laterally positioned cameras (100 Hz) by tracking the orientation of an ellipse fit to each pupil (Figure 3B; see STAR Methods).

All birds were able to simultaneously compensate for visual motion simulating both backward (NT-NT) and forward (TN-TN) translation (Figures 3C and 3D, respectively) through eye-in-head movements. Pigeons tracked visual motion regardless of the direction of stimuli shown to the opposite eye and kept their eyes stable during stationary stimuli (Figure 3E).

In outdoor trials, flying pigeons exhibited slow temporal eye movements (Figures 1N–1R). These head-restrained experiments using simulated optic flow demonstrated that pigeons can simultaneously stabilize temporal optic flow displayed to both eyes (Figure 3C). Thus, the monocular pattern of temporal eye movements that we characterized during free flight likely represents a binocular pattern of divergent eye movements. As these slow eye movements were consistent with the speed and direction of optic flow along the horizon in the lateral visual fields (Figures 2I and 2J), we propose that pigeons exhibit a divergent optokinetic response to optic flow during flight.

Pigeons make large convergent eye movements when landing

Finally, we revisited a pattern of oculomotor behavior apparent during landing, during which there was a large and consistent change in eye position (Figure 4A; Video S1). Specifically, for the period 1–0.25s prior to substrate contact, the eye shifted an average of 5.4° ± 2.3° forward and 2.5° ± 1.7° downward

Please cite this article in press as: Lapsansky et al., Pigeons make slow, divergent eye movements during flight and large, convergent eye movements when landing, Current Biology (2026), https://doi.org/10.1016/j.cub.2026.06.015

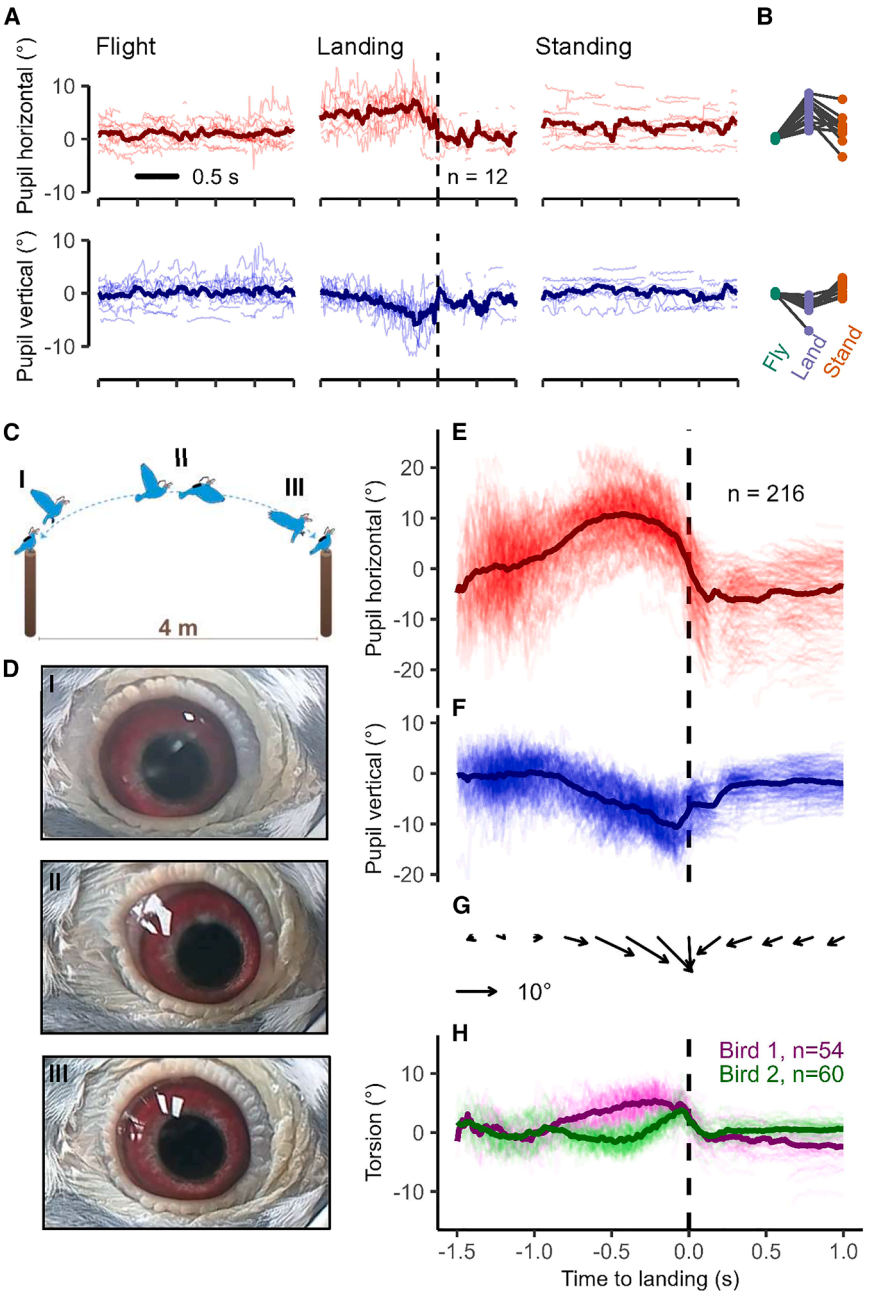

Figure 4. Pigeons converge their eyes during landing, suggesting frontal fixation

(A) Representative horizontal (top) and vertical (bottom) eye position for 2.5 s of homing flight, landing, and standing outside in the field (n = 12). Vertical dashed line indicates the timing of substrate contact. Positive is dorsal/nasal, and negative is ventral/temporal.

(B) Mean horizontal (top) and vertical (bottom) eye position during homing flight, landing (1–0.25 s prior to substrate contact), and standing. The eye tended to shift nasal and down prior to landing.

(C) To test if this pattern is stereotypical of landing, pigeons (n = 3) were trained to fly repeatedly between two perches indoors, spaced 4 m apart.

(D) Representative frames from a single perch-to-perch flight, I. pre-takeoff, II. flight/landing, and III. post-landing. Note the ventro-nasal offset in eye position and, also, the increased visibility of the temporo-dorsal sclera at II. flight/landing.

(E and F) (E) Horizontal and (F) vertical eye positions for 216 landings, aligned to the timing of substrate contact (t = 0). Dark lines are the mean position at each time step.

(G) The relative vector sum of the horizontal and vertical eye position suggests fixation on the point of landing.

(H) Torsional eye position for two individuals with trackable iris features. Timing of torsion differed between individuals, but both exhibited intorsion on their approach to the perch, consistent with fixation. See also Figure S1 and Video S4.

(Figure 4B). However, this pattern was based on few landings (n = 12) as the camera often collided with the wings.

To better understand eye movements during landing, we trained pigeons (n = 3) to make repeated perch-to-perch flights (n = 216) within an indoor flight arena while recording eye position (Figures 4C and 4D; Video S4). In addition to horizontal and vertical eye position, for two birds with conspicuous iris features, we also measured torsional eye movements. Averaging position across landings by time, maximum deflections of 10.8° forward (Figure 4E) and 10.7° downward (Figure 4F) occurred 433 ms and 89 ms prior to perch contact for these short flights. Computing the vector sum of trial-averaged horizontal and vertical eye positions through time suggests that pigeons use eye-in-head movements to maintain a stable image of the perch during approach (Figure 4G). Both birds for which we could measure torsional eye position consistently rotated the top margin of their eyes in the nasal direction (intorsion) by a maximum of 4.1° at 56 ms prior to perch contact, though the dynamics of these movements varied between individuals (Figure 4H).

DISCUSSION

Although eye movements have been considered insignificant during avian flight,[8,35–37] we conclude that pigeons use slow, divergent eye movements during flight and large, convergent movements during landing. The divergent movements were consistent with an optokinetic response—eye movements that minimize image slip—to optic flow in the lateral visual fields along the horizon. We base this conclusion on the following evidence: (1) during flight, pigeons exhibit primarily temporal eye movements with little to no vertical component (Figures 1O–1Q); (2) in the lateral visual fields along the horizon, optic flow is nearly always temporally directed and of similar speed to the slow eye movements (Figures 2I and 2J); (3) above the horizon, optic flow contains a small but clear upward component (Figure 2H); (4) below the horizon, optic flow contains a strong downward component

Please cite this article in press as: Lapsansky et al., Pigeons make slow, divergent eye movements during flight and large, convergent eye movements when landing, Current Biology (2026), https://doi.org/10.1016/j.cub.2026.06.015

(Figure 2H); and (5) under laboratory conditions, pigeons stabilize temporal optic flow at similar speeds using binocular, divergent eye movements (Figures 3D and 3E). Though the number of animals in our study is somewhat small due to the challenges associated with recording from free-moving pigeons, these patterns were highly stereotyped.

Optokinetic responses during locomotion have been considered maladaptive,[16,38] as they distort the optic flow field and thereby complicate guidance; however, they may also provide perceptual benefits. Because birds exhibit remarkable head stabilization during flight,[8,39–41] without optokinetic eye movements, stationary features, such as navigational landmarks,[42] would blur due to image motion produced by the translation of a stable head. Moving objects, such as predators or flock mates, are also easier to detect against a stable background.[25] Slow, divergent eye movements may therefore increase the saliency of visual information critical for flight.

Importantly, because the optic flow field during translation is not uniform (Figures 2G and 2H), stabilizing any single region does not eliminate visual motion elsewhere. Stabilizing the lateral visual field through the optokinetic response, which is driven by retinal ganglion cells distributed across the retina,[43,44] has the added benefit of also stabilizing the lateral fovea, which feeds the tectofugal and thalamofugal pathways for object identification.[45,46] However, other regions of the retina will still experience retinal slip that could be used for other aspects of flight control, including obstacle avoidance and navigation.[20,47,48]

During landing, pigeons made large, convergent eye movements (Figure 4). Peahens also make similar convergent eye movements when jumping.[49] Potentially, convergence could allow for stereopsis based on retinal disparity cues.[50] The pigeon retina contains two regions of high visual acuity—the lateral fovea, projecting to the sides of the animal, and the *area dorsalis*, projecting down and forward.[51,52] During feeding bouts, pigeons shift their eyes forward by ~12°, presumably to attain a higher-resolution, binocular view of food items by bringing the *area dorsalis* of each eye into register.[53,54] These shifts scale during pecking with the distance between the eye and the food item,[55] similar to what we observed during landing (Figure 4G). Importantly, binocular fixation does not require stereopsis.[50,56] Pigeons can peck and land accurately even when one eye is covered.[55,57] Instead, convergence could cause the optic flow field to expand more symmetrically around the perch, improving guidance[58] and perception of time to collision.[59] Importantly, we do not reconstruct gaze during landing and instead infer perch fixation based on the similarity between these eye movements and those during feeding.[53,54]

As technology continues to improve,[60,61] we anticipate more studies will use head orientation and position—through head-mounted cameras and sensors—to track flying birds. This work demonstrates that eye movements for shifting and stabilizing gaze during flight are not insignificant. Given their small size, however, if the goal is to document visual attention,[62] then head orientation should be sufficiently accurate, at least outside of landing. If the goal is related to perception of optic flow or visual pursuit, then researchers should carefully consider how eye movements modify visual motion occurring at the retina.

RESOURCE AVAILABILITY

Lead contact

Requests for further information and resources should be directed to and will be fulfilled by the lead contact, Douglas L. Altshuler (doug.altshuler@ubc.ca).

Materials availability

This study did not generate any new, unique materials.

Data and code availability

- Raw and processed data have been deposited at Dryad as DOI: 10.5061/dryad.3j9kd51zx and are publicly available as of the date of publication.
- All original code has been deposited at Dryad and is publicly available at DOI: 10.5061/dryad.3j9kd51zx as of the date of publication.
- Any additional information required to reanalyze the data reported in this paper is available from the lead contact upon request.

ACKNOWLEDGMENTS

We acknowledge Nick Tochor and Bhaskar Yechuri for developing initial prototypes of the camera system. Suryadeep Dash and Philipp Kreyenmeier provided guidance on the analysis of eye movement data. We thank Vikram Baliga, Eric Press, Jolan Theriault, Jasmin Wong, and Francesca Ciocca for helpful comments on an early version of this manuscript. This work was funded by the Michael Smith Health Research BC/Parkinson Society, British Columbia (RT−2023–3226) to A.B.L., the National Science Foundation (2109873) to A.B.L., and a Discovery Grant (RGPIN−2021–02977) from the Natural Sciences and Engineering Research Council of Canada to D.L.A. Support for A.B.L. was also provided by the National Science Foundation (2332837).

AUTHOR CONTRIBUTIONS

Conceptualization: A.B.L., D.R.W., and D.L.A.; methodology: A.B.L.; software: A.B.L.; validation: A.B.L., D.R.W., and D.L.A.; formal analysis: A.B.L.; investigation: A.B.L.; resources: A.B.L. and D.L.A.; data curation: A.B.L.; writing – original draft: A.B.L. and D.L.A.; writing – review & editing: A.B.L., D.R.W., and D.L.A.; visualization: A.B.L.; supervision: D.R.W. and D.L.A.; project administration: A.B.L., D.R.W., and D.L.A.; funding acquisition: A.B.L., D.R.W., and D.L.A.

DECLARATION OF INTERESTS

The authors declare no competing interests.

DECLARATION OF GENERATIVE AI AND AI-ASSISTED TECHNOLOGIES IN THE WRITING PROCESS

During the preparation of this work, the author(s) used ChatGPT in order to detect spelling errors and typos and suggest suitable functions for analysis. After using this tool or service, we reviewed and edited the content as needed and take full responsibility for the content of the publication.

STAR★METHODS

Detailed methods are provided in the online version of this paper and include the following:

- KEY RESOURCES TABLE
- EXPERIMENTAL MODEL AND STUDY PARTICIPANT DETAILS
- METHOD DETAILS
  - Eye and optic flow tracking equipment
  - Experimental procedure
  - Data processing
  - Eye tracking
  - Calibration of eye tracking system

- Binocular oculomotor response to translational optic flow
- Optic flow tracking
- QUANTIFICATION AND STATISTICAL ANALYSIS

SUPPLEMENTAL INFORMATION

Supplemental information can be found online at https://doi.org/10.1016/j.cub.2026.06.015.

Received: April 27, 2026
Revised: May 28, 2026
Accepted: June 8, 2026

REFERENCES

1. Gibson, J.J. (1950). The Perception of the Visual World (Houghton Mifflin Company).
2. Srinivasan, M.V. (2014). Going with the flow: a brief history of the study of the honeybee's navigational 'odometer.'. J. Comp. Physiol. A Neuroethol. Sens. Neural Behav. Physiol. *200*, 563–573. https://doi.org/10.1007/s00359-014-0902-6.
3. Angelaki, D.E., and Hess, B.J.M. (2005). Self-motion-induced eye movements: effects on visual acuity and navigation. Nat. Rev. Neurosci. *6*, 966–976. https://doi.org/10.1038/nrn1804.
4. Westheimer, G., and McKee, S.P. (1975). Visual acuity in the presence of retinal-image motion. J. Opt. Soc. Am. *65*, 847–850. https://doi.org/10.1364/josa.65.000847.
5. Nakayama, K. (1985). Biological image motion processing: a review. Vis. Res. *25*, 625–660. https://doi.org/10.1016/0042-6989(85)90171-3.
6. Wallman, J., and Letelier, J.-C. (1993). Eye movements, head movements, and gaze stabilization in birds. In Vision, Brain, and Behavior in Birds (The MIT Press), pp. 245–263.
7. Land, M.F. (2015). Eye movements of vertebrates and their relation to eye form and function. J. Comp. Physiol. A Neuroethol. Sens. Neural Behav. Physiol. *201*, 195–214. https://doi.org/10.1007/s00359-014-0964-5.
8. Kano, F., Walker, J., Sasaki, T., and Biro, D. (2018). Head-mounted sensors reveal visual attention of free-flying homing pigeons. J. Exp. Biol. *221*, jeb183475. https://doi.org/10.1242/jeb.183475.
9. Lapsansky, A.B., Kreyenmeier, P., Spering, M., Wylie, D.R., and Altshuler, D.L. (2025). Hummingbirds use compensatory eye movements to stabilize both rotational and translational visual motion. Proc. Biol. Sci. *292*, 20242015. https://doi.org/10.1098/rspb.2024.2015.
10. Mathis, A., Mamidanna, P., Cury, K.M., Abe, T., Murthy, V.N., Mathis, M.W., and Bethge, M. (2018). DeepLabCut: markerless pose estimation of user-defined body parts with deep learning. Nat. Neurosci. *21*, 1281–1289. https://doi.org/10.1038/s41593-018-0209-y.
11. Erichsen, J.T., Hodos, W., Evinger, C., Bessette, B.B., and Phillips, S.J. (1989). Head orientation in pigeons: postural, locomotor and visual determinants. Brain Behav. Evol. *33*, 268–278. https://doi.org/10.1159/000115935.
12. Sibley, D.A. (2016). Sibley Birds West: Field Guide to Birds of Western North America (Knopf Publishing Group).
13. Bloch, S., Rivaud, S., and Martinoya, C. (1984). Comparing frontal and lateral viewing in the pigeon. III. Different patterns of eye movements for binocular and monocular fixation. Behav. Brain Res. *13*, 173–182. https://doi.org/10.1016/0166-4328(84)90147-5.
14. Gandhi, N.J., and Katnani, H.A. (2011). Interactions of eye and eyelid movements. In The Oxford Handbook of Eye Movements, S.P. Liversedge, I. Gilchrist, and S. Everling, eds. (Oxford University Press). https://doi.org/10.1093/oxfordhb/9780199539789.013.0017.
15. Binda, P., and Morrone, M.C. (2018). Vision during saccadic eye movements. Annu. Rev. Vis. Sci. *4*, 193–213. https://doi.org/10.1146/annurev-vision-091517-034317.
16. Collewijn, H., and Noorduin, H. (1972). Conjugate and disjunctive optokinetic eye movements in the rabbit, evoked by rotatory and translatory motion. Pflugers Arch. *335*, 173–185. https://doi.org/10.1007/BF00592155.
17. Serres, J.R., Evans, T.J., Åkesson, S., Duriez, O., Shamoun-Baranes, J., Ruffier, F., and Hedenström, A. (2019). Optic flow cues help explain altitude control over sea in freely flying gulls. J. R. Soc. Interface *16*, 20190486. https://doi.org/10.1098/rsif.2019.0486.
18. Lee, D.N., Kalmus, H., Longuet-Higgins, H.C., and Sutherland, N.S. (1980). The optic flow field: the foundation of vision. Philos. Trans. R. Soc. Lond., B Biol. Sci. *290*, 169–179. https://doi.org/10.1098/rstb.1980.0089.
19. Krapp, H.G. (2013). Optic flow processing. In Encyclopedia of Computational Neuroscience, D. Jaeger, and R. Jung, eds. (Springer), pp. 1–22. https://doi.org/10.1007/978-1-4614-7320-6_332-1.
20. Bhagavatula, P.S., Claudianos, C., Ibbotson, M.R., and Srinivasan, M.V. (2011). Optic Flow Cues Guide Flight in Birds. Curr. Biol. *21*, 1794–1799. https://doi.org/10.1016/j.cub.2011.09.009.
21. Fry, S.N., Rohrseitz, N., Straw, A.D., and Dickinson, M.H. (2009). Visual control of flight speed in *Drosophila melanogaster*. J. Exp. Biol. *212*, 1120–1130. https://doi.org/10.1242/jeb.020768.
22. Gioanni, H., Rey, J., Villalobos, J., Bouyer, J.J., and Gioanni, Y. (1981). Optokinetic nystagmus in the pigeon (*Columba livia*): I. Study in monocular and binocular vision. Exp. Brain Res. *44*, 362–370. https://doi.org/10.1007/BF00238829.
23. Fenk, L.M., Avritzer, S.C., Weisman, J.L., Nair, A., Randt, L.D., Mohren, T.L., Siwanowicz, I., and Maimon, G. (2022). Muscles that move the retina augment compound eye vision in *Drosophila*. Nature *612*, 116–122. https://doi.org/10.1038/s41586-022-05317-5.
24. Mei Chow, H., and Spering, M. (2023). Eye movements during optic flow perception. Vis. Res. *204*, 108164. https://doi.org/10.1016/j.visres.2022.108164.
25. Land, M.F. (1999). Motion and vision: why animals move their eyes. J. Comp. Physiol. A *185*, 341–352. https://doi.org/10.1007/s003590050393.
26. Walls, G.L. (1962). The evolutionary history of eye movements. Vis. Res. *2*, 69–80. https://doi.org/10.1016/0042-6989(62)90064-0.
27. Nakayama, K. (1981). Differential motion hyperacuity under conditions of common image motion. Vis. Res. *21*, 1475–1482. https://doi.org/10.1016/0042-6989(81)90218-2.
28. Eckmeier, D., Geurten, B.R.H., Kress, D., Mertes, M., Kern, R., Egelhaaf, M., and Bischof, H.-J. (2008). Gaze Strategy in the Free Flying Zebra Finch (*Taeniopygia guttata*). PLoS One *3*, e3956. https://doi.org/10.1371/journal.pone.0003956.
29. Collewijn, H. (1977). Eye- and head movements in freely moving rabbits. J. Physiol. *266*, 471–498. https://doi.org/10.1113/jphysiol.1977.sp011778.
30. Necker, R. (2007). Head-bobbing of walking birds. J. Comp. Physiol. A Neuroethol. Sens. Neural Behav. Physiol. *193*, 1177–1183. https://doi.org/10.1007/s00359-007-0281-3.
31. Clark, W., and Colombo, M. (2022). Seeing the Forest for the Trees, and the Ground Below My Beak: Global and Local Processing in the Pigeon's Visual System. Front. Psychol. *13*, 888528. https://doi.org/10.3389/fpsyg.2022.888528.
32. Snyder, J.P. (1987). Map projections: A working manual Professional Paper (U.S. Government Printing Office). https://doi.org/10.3133/pp1395.
33. Yorzinski, J.L. (2016). Eye blinking in an avian species is associated with gaze shifts. Sci. Rep. *6*, 32471. https://doi.org/10.1038/srep32471.

34. Stickney, K.J., Donahoe, J.W., and Carlson, N.R. (1981). Conditioning preparation for the nictitating membrane of the pigeon. Behav. Res. Methods Instrum. *13*, 653–656. https://doi.org/10.3758/BF03202082.

35. Brighton, C.H., Thomas, A.L.R., and Taylor, G.K. (2017). Terminal attack trajectories of peregrine falcons are described by the proportional navigation guidance law of missiles. Proc. Natl. Acad. Sci. USA. *114*, 13495–13500. https://doi.org/10.1073/pnas.1714532114.

36. Kempton, J.A., Brighton, C.H., France, L.A., KleinHeerenbrink, M., Miñano, S., Shelton, J., and Taylor, G.K. (2023). Visual versus visual-inertial guidance in hawks pursuing terrestrial targets. J. R. Soc. Interface *20*, 20230071. https://doi.org/10.1098/rsif.2023.0071.

37. Ros, I.G., Bhagavatula, P.S., and Biewener, A.A. (2026). Pigeons lock their eyes in place during flight. Curr. Biol. *36*, 1–7. https://doi.org/10.1016/j.cub.2026.05.064.

38. Easter, S.S. (1972). Pursuit eye movements in goldfish (*Carassius auratus*). Vis. Res. *12*, 673–688. https://doi.org/10.1016/0042-6989(72)90161-7.

39. Ros, I.G., and Biewener, A.A. (2017). Pigeons (*C. livia*) Follow Their Head during Turning Flight: Head Stabilization Underlies the Visual Control of Flight. Front. Neurosci. *11*, 655. https://doi.org/10.3389/fnins.2017.00655.

40. Kress, D., van Bokhorst, E., and Lentink, D. (2015). How Lovebirds Maneuver Rapidly Using Super-Fast Head Saccades and Image Feature Stabilization. PLoS One *10*, e0129287. https://doi.org/10.1371/journal.pone.0129287.

41. Warrick, D.R., Bundle, M.W., and Dial, K.P. (2002). Bird Maneuvering Flight: Blurred Bodies, Clear Heads. Integr. Comp. Biol. *42*, 141–148. https://doi.org/10.1093/icb/42.1.141.

42. Vyssotski, A.L., Dell'Omo, G., Dell'Ariccia, G., Abramchuk, A.N., Serkov, A.N., Latanov, A.V., Loizzo, A., Wolfer, D.P., and Lipp, H.-P. (2009). EEG Responses to Visual Landmarks in Flying Pigeons. Curr. Biol. *19*, 1159–1166. https://doi.org/10.1016/j.cub.2009.05.070.

43. Karten, J.H., Fite, K.V., and Brecha, N. (1977). Specific projection of displaced retinal ganglion cells upon the accessory optic system in the pigeon (*Columba livia*). Proc. Natl. Acad. Sci. USA. *74*, 1753–1756. https://doi.org/10.1073/pnas.74.4.1753.

44. Wylie, D.R., Kolominsky, J., Graham, D.J., Lisney, T.J., and Gutierrez-Ibanez, C. (2014). Retinal projection to the pretectal nucleus lentiformis mesencephali in pigeons (*Columba livia*). J. Comp. Neurol. *522*, 3928–3942. https://doi.org/10.1002/cne.23649.

45. Clark, W.J., and Colombo, M. (2020). The functional architecture, receptive field characteristics, and representation of objects in the visual network of the pigeon brain. Prog. Neurobiol. *195*, 101781. https://doi.org/10.1016/j.pneurobio.2020.101781.

46. Wylie, D.R.W., Gutierrez-Ibanez, C., Pakan, J.M.P., and Iwaniuk, A.N. (2009). The optic tectum of birds: Mapping our way to understanding visual processing. Can. J. Exp. Psychol. *63*, 328–338. https://doi.org/10.1037/a0016826.

47. Williams, C.D., and Biewener, A.A. (2015). Pigeons trade efficiency for stability in response to level of challenge during confined flight. Proc. Natl. Acad. Sci. USA. *112*, 3392–3396. https://doi.org/10.1073/pnas.1407298112.

48. Alexander, E., Cai, L.T., Fuchs, S., Hladnik, T.C., Zhang, Y., Subramanian, V., Guilbeault, N.C., Vijayakumar, C., Arunachalam, M., Juntti, S.A., et al. (2022). Optic flow in the natural habitats of zebrafish supports spatial biases in visual self-motion estimation. Curr. Biol. *32*, 5008–5021.e8. https://doi.org/10.1016/j.cub.2022.10.009.

49. Yorzinski, J.L. (2019). Conjugate eye movements guide jumping locomotion in an avian species. J. Exp. Biol. *222*, jeb211565. https://doi.org/10.1242/jeb.211565.

50. McFadden, S.A., and Wild, J.M. (1986). Binocular Depth Perception in the Pigeon. J. Exp. Anal. Behav. *45*, 149–160. https://doi.org/10.1901/jeab.1986.45-149.

51. Binggeli, R.L., and Paule, W.J. (1969). The pigeon retina: Quantitative aspects of the optic nerve and ganglion cell layer. J. Comp. Neurol. *137*, 1–18. https://doi.org/10.1002/cne.901370102.

52. Galifret, Y. (1968). Les diverses aires fonctionnelles de la rétine du Pigeon. Z. Zellforsch. Mikrosk. Anat. *86*, 535–545. https://doi.org/10.1007/BF00324864.

53. Wohlschläger, A., Jäger, R., and Delius, J.D. (1993). Head and eye movements in unrestrained pigeons (*Columba livia*). J. Comp. Psychol. *107*, 313–319. https://doi.org/10.1037/0735-7036.107.3.313.

54. Nalbach, H.O., Wolf-Oberhollenzer, F., and Kirschfeld, K. (1990). The pigeon's eye viewed through an ophthalmoscopic microscope: Orientation of retinal landmarks and significance of eye movements. Vis. Res. *30*, 529–540. https://doi.org/10.1016/0042-6989(90)90065-S.

55. Martinoya, C., Le Houezec, J., and Bloch, S. (1984). Pigeon's eyes converge during feeding: Evidence for frontal binocular fixation in a lateral-eyed bird. Neurosci. Lett. *45*, 335–339. https://doi.org/10.1016/0304-3940(84)90248-9.

56. Martinoya, C., Le Houezec, J., and Bloch, S. (1988). Depth resolution in the pigeon. J. Comp. Physiol. A *163*, 33–42. https://doi.org/10.1007/BF00611994.

57. Martinho, A., Biro, D., Guilford, T., Gagliardo, A., and Kacelnik, A. (2015). Asymmetric visual input and route recapitulation in homing pigeons. Proc. Biol. Sci. *282*, 20151957. https://doi.org/10.1098/rspb.2015.1957.

58. Martin, G.R. (2009). What is binocular vision for? A birds' eye view. J. Vis. *9*, 14.1–1419. https://doi.org/10.1167/9.11.14.

59. Wang, Y., and Frost, B.J. (1992). Time to collision is signalled by neurons in the nucleus rotundus of pigeons. Nature *356*, 236–238. https://doi.org/10.1038/356236a0.

60. Tanigaki, K., Otsuka, R., Li, A., Hatano, Y., Wei, Y., Koyama, S., Yoda, K., and Maekawa, T. (2024). Automatic recording of rare behaviors of wild animals using video bio-loggers with on-board light-weight outlier detector. PNAS Nexus *3*, pgad447. https://doi.org/10.1093/pnasnexus/pgad447.

61. Dunn, R.E., Trevail, A.M., Nicoll, M.A.C., Freeman, R., Braman, C.A., Clark, B.L., Mitchell, C., Schiffmiller, A.W., Wood, H., and Votier, S.C. (2025). Commuting in crosswinds and foraging in fast winds: the foraging ecology of a flying fish specialist. Proc. Biol. Sci. *292*, 20250774. https://doi.org/10.1098/rspb.2025.0774.

62. Kano, F., Naik, H., Keskin, G., Couzin, I.D., and Nagy, M. (2022). Head-tracking of freely-behaving pigeons in a motion-capture system reveals the selective use of visual field regions. Sci. Rep. *12*, 19113. https://doi.org/10.1038/s41598-022-21931-9.

63. Sargisson, R.J., McLean, I.G., Brown, G.S., and White, K.G. (2007). Seasonal Variation in Pigeon Body Weight and Delayed Matching-to-Sample Performance. J. Exp. Anal. Behav. *88*, 395–404. https://doi.org/10.1901/jeab.2007.88-395.

64. Portugal, S.J., and White, C.R. (2022). Externally attached biologgers cause compensatory body mass loss in birds. Methods Ecol. Evol. *13*, 294–302. https://doi.org/10.1111/2041-210X.13754.

65. Ricketts, R.L., Sankey, D.W.E., Tidswell, B.P., Brown, J., Deegan, J.F., and Portugal, S.J. (2022). Overall dynamic body acceleration as an indicator of dominance in Homing Pigeons (*Columba livia*). Ibis *164*, 581–586. https://doi.org/10.1111/ibi.13021.

66. Crawford, E.C., and Kampe, G. (1971). Resonant panting in pigeons. Comp. Biochem. Physiol. A Comp. Physiol. *40*, 549–552. https://doi.org/10.1016/0300-9629(71)90048-X.

67. Lewden, A., Bishop, C.M., and Askew, G.N. (2023). How birds dissipate heat before, during and after flight. J. R. Soc. Interface *20*, 20230442. https://doi.org/10.1098/rsif.2023.0442.

68. Schwarz, J.S., Sridharan, D., and Knudsen, E.I. (2013). Magnetic tracking of eye position in freely behaving chickens. Front. Syst. Neurosci. *7*, 91. https://doi.org/10.3389/fnsys.2013.00091.

69. Juhola, M. (1991). Median filtering is appropriate to signals of saccadic eye movements. Comput. Biol. Med. *21*, 43–49. https://doi.org/10.1016/0010-4825(91)90034-7.

70. Maechtle, T. (1998). The Aba: A Device for restraining raptors and other large birds. J. Field Ornithol. *69*, 66–70.

71. Alvarez, L., Gómez, L., and Sendra, J.R. (2009). An Algebraic Approach to Lens Distortion by Line Rectification. J. Math. Imaging Vis. *35*, 36–50. https://doi.org/10.1007/s10851-009-0153-2.

72. Bukhari, F., and Dailey, M.N. (2013). Automatic Radial Distortion Estimation from a Single Image. J. Math. Imaging Vis. *45*, 31–45. https://doi.org/10.1007/s10851-012-0342-2.

73. Ettinger, S.M., Nechyba, M.C., Ifju, P.G., and Waszak, M. (2003). Vision-guided flight stability and control for micro air vehicles. Adv. Robot. *17*, 617–640. https://doi.org/10.1163/156855303769156983.

74. Kroeger, T., Timofte, R., Dai, D., and Van Gool, L. (2016). Fast Optical Flow Using Dense Inverse Search. In Computer Vision – ECCV, B. Leibe, J. Matas, N. Sebe, and M. Welling, eds. (Springer International Publishing), pp. 471–488. https://doi.org/10.1007/978-3-319-46493-0_29.

75. Schroder, G., Senst, T., Bochinski, E., and Sikora, T. (2018). Optical Flow Dataset and Benchmark for Visual Crowd Analysis. In 15th IEEE International Conference on Advanced Video and Signal Based Surveillance (AVSS), pp. 1–6. https://doi.org/10.1109/AVSS.2018.8639113.

Please cite this article in press as: Lapsansky et al., Pigeons make slow, divergent eye movements during flight and large, convergent eye movements when landing, Current Biology (2026), https://doi.org/10.1016/j.cub.2026.06.015

CellPress

STAR★METHODS

KEY RESOURCES TABLE

REAGENT or RESOURCE	SOURCE	IDENTIFIER
Deposited data		
Data analysis code in MATLAB, Python, and R	Dryad	10.5061/dryad.3j9kd51zx
Raw eye data	Dryad	10.5061/dryad.3j9kd51zx
Raw optic flow data	Dryad	10.5061/dryad.3j9kd51zx
Video data	Dryad	10.5061/dryad.3j9kd51zx
Experimental models: organisms/strains		
Homing pigeon, *Columba livia domestica*	Local hobbyist	N/A
Software and algorithms		
R version 4.4.1	R	https://www.r-project.org/
DeepLabCut	Mathis et al.[10]	https://github.com/deeplabcut/deeplabcut
Python V 3.12.4	Python	https://www.python.org/
MATLAB R2024a	Mathworks Inc.	https://www.mathworks.com/products/new_products/release2024a.html
Other		
Raspberry Pi Zero 2 W	Adafruit	https://www.adafruit.com/product/5291
Adafruit LSM6DSOX + LIS3MDL	Adafruit	https://www.adafruit.com/product/4517
Mini size Camera 5MP OV5647 sensor, MELIFE – 30 CM	Amazon	ASIN B092Z9M5V3
350 mAh battery	Adafruit	https://www.adafruit.com/product/2750
TrackPack	Marshall Radio Telemetry	https://marshallradio.com/ww/product/trackpack-mounting-system/
HD14F 1021 lens, 1.0 mm focal length	Aliexpress	HD14F1021

EXPERIMENTAL MODEL AND STUDY PARTICIPANT DETAILS

All procedures were approved by the University of British Columbia Animal Care Committee in accordance with the guidelines set out by the Canadian Council on Animal Care. Homing pigeons (*Columba livia domestica*) were provided by a local breeder (Ferndale, Washington, USA), who was responsible for maintenance and care. We did not determine the sex of animals involved in this study, as this is notoriously difficult in pigeons.

All eye tracking and optic flow flights occurred back to their natal home loft. Birds were transported in plastic pigeon baskets that allowed for light and airflow secured to the bed of a vehicle. Pigeons were always released in groups of 10–16 to provide some protection from local predators. Pigeons were selected for inclusion in the study based on recommendations from the breeder and their immediate return to the home loft during test flights from the distant release site (2.05 km north of home loft). The release site was chosen as the closest accessible open field, wherein we could visually scan for predators before release. These birds were fitted with backpacks and allowed to move freely around the loft for 2 hours under constant observation for signs of discomfort and abnormal patterns of locomotion. Adjustments to backpack fit were made as needed.

Once properly fit, we allowed pigeons to acclimate for 1–2 weeks to the unweighted backpack, during which we continued to release them at least every other day from the release site. After this, we fit each bird with "mock" equipment, consisting of a steel

Please cite this article in press as: Lapsansky et al., Pigeons make slow, divergent eye movements during flight and large, convergent eye movements when landing, Current Biology (2026), https://doi.org/10.1016/j.cub.2026.06.015

bar the approximate mass and size of the camera system, and allowed an additional 1–2 weeks of acclimation during which we continued training flights. Pigeons that failed to return immediately from training flights were dropped from the study. Each study bird was also fitted with a specific mask. We attached the mask and allowed the bird to move freely around the loft for 2 hours under constant observation for signs of discomfort and abnormal patterns of locomotion.

METHOD DETAILS

Eye and optic flow tracking equipment

Our system for recording eye movement (Figure 1A) and optic flow (Figure 3A) was based on the Raspberry Pi Zero 2 single-board computer (Raspberry Pi Foundation, Cambridge, England, UK). Inertial data (80 Hz) were provided by combination LSM6DSOX + LIS3MDL – Precision 9 DoF IMUs (Adafruit, New York, New York, USA). Cameras (~90 Hz, 640 x 480 pixels) utilized a 5 MP OV5647 sensor with a 30 cm FFC sold by "MELIFE" through Amazon (Seattle, WA, USA). Videos were saved in H.264 format to a microSD card using the *picamera* library with the exposure mode set to "sports" to minimize motion blur. Systems were each powered by a single lithium-ion battery (350–450 mAh) manufactured by Shenzhen PKCell Battery Co. LTD (Shenzhen, China). These components were connected and wrapped in wire-harness tape to protect the bird from any sharp edges.

All parts of the system aside from the camera and lens were attached to a backpack constructed of Velcro (Manchester, New Hampshire, USA) with straps made from Teflon tubular ribbon (TrackPack, Marshall Radio Telemetry, North Salt Lake, Utah, USA). The total mass of this equipment varied depending on the amount of tape and averaged around 30 g (6%–9% of body mass, depending on the animal). Less than 3 g of this mass were on the head. The system was capable of recording for ~25 min, depending on the size of battery and outdoor temperature. Due to weight and power limitations, we were unable to include a GPS in these trials. We also attempted to include a high-speed IMU on the head, but this proved problematic due to multiple cables running from the backpack to the head and the added mass on the head.

It is likely that a 30 g mass affects some aspects of pigeon flight that were not evaluated. However, it is important that only 3 g were attached to the head of the bird, and the total equipment mass represents an additional 6%–9% of body mass. This addition is within the range of natural body mass fluctuations of pigeons.[63] Also, pigeons equipped with added mass will lose body mass within a few weeks to compensate for artificial loading.[64]

The camera and lens were attached to custom-fitted masks made from leather, similar to traditional Dutch falconry hoods but with the side panels removed (Figure 1A). For eye tracking, the camera was attached via a semi-flexible metal arm (Figure 1B). This metal arm allowed us to adjust the camera orientation to align with the optical axis of the focal eye just before release and prevent injury to the pigeon if the camera were to collide with a solid object. For recording optic flow, the camera was attached directly to the mask via cyanoacrylate glue and oriented along the optical axis of the eye (Figure 3A)—60° lateral from straight forward.[31] This orientation was confirmed by photographing the attached camera and mask from above just before release. The total mass on the head was <3 g.

Cameras came equipped with lenses having fields of view of 70°. To confirm that the lower eye ring aligned with horizontal,[11] we manually replaced the lens of a single camera with a 120° lens from a separate camera and used this for a portion of flights (5 flights, 2 birds). Given our method of calibration (see *Eye tracking* and *Calibration of eye tracking camera* sections below) this wider field of view does not impact our measurement of eye position. For optic flow recordings, we replaced lenses with wide-angle lenses having a focal length of 1.0 mm (Huidongbao, Shenzhen, CN).

Experimental procedure

We recorded data for a given bird after successful acclimation and fit testing. Training flights were intended to ensure that birds knew the route home and would spend less time circling the release site, where they were vulnerable to predators. Equipped birds were released alongside 8–14 other pigeons, typically with one other equipped bird and 3–6 individuals with "mock" equipment. As we continued to train non-equipped birds while recording data from others, the number of training flights ranged from 10 to 30 depending on the bird. All outdoor flights were conducted between July and August of 2022. A wider set of animals was used for optic flow flights, as we found that more animals were amenable to this equipment than the eye tracking setup.

Outdoor eye tracking and optic flow flights occurred back to the pigeon home loft, either from a distant release site or from just outside the home loft (3 eye tracking flights from 3 birds, released <100 m from home loft). These latter flights were intended to test equipment and are included to increase the amount of data for standing for those individuals. We attempted to obtain data for three complete flights from the distant release site for each individual included in the study. Some birds were removed after one or two flights because they chose to land rather than immediately return home, increasing risk of predation. Rather than risk their safety, we opted to switch to a different bird that had completed all training flights with the "mock" weight. Such behavioral variation is a known feature when training homing pigeons.

On the day of recording, focal birds were transported to the release site along with conspecifics. Their "mock" weight was removed and immediately replaced with the camera system. Systems were configured to start recording video and inertial data upon power up. The hood was attached and inspected to ensure proper fit. Then, focal birds were placed in a release container. This container was opened alongside one containing conspecifics so that equipped birds could leave voluntarily alongside their flock-mates. Birds that failed to leave voluntarily were not released. After birds left their containers, we returned to the home loft, often arriving after the flock. Once equipped birds entered the loft, we retrieved the camera equipment and replaced it with "mock" equipment before downloading video and inertial data.

Please cite this article in press as: Lapsansky et al., Pigeons make slow, divergent eye movements during flight and large, convergent eye movements when landing, Current Biology (2026), https://doi.org/10.1016/j.cub.2026.06.015

Data processing

We processed data using a combination of Python (V 3.12.4) and MATLAB R2024a (MathWorks Inc., Natick, Massachusetts, USA). To enable high frame rates, videos were recorded as H.264 video streams, which lack timecode information. For this reason, inertial data were saved alongside the system time, which was also burned into the lower margin of each frame (Figures 1C and 3B). These timestamps were beyond the margins of data analyzed for both eye tracking and optic flow videos. Videos in H.264 were converted to MKV video format with a framerate of 90 Hz for ease of use. However, timestamps were extracted from each video frame via optical text recognition in Python and were used to synchronize the two data streams using MATLAB.

We used gyroscope data to automatically categorize data by behavior—flying, landing, walking, and standing (Figure 1E), though we visually checked all flights manually. For each flight, we first removed minor gyroscope bias measured when the sensor was motionless on a flat and stable surface. These IMUs had exceptionally low values of bias and any fixed offset would not affect our method of categorizing behavior, as our thresholds were based on visual inspection of both IMU signal and video data.

We then synchronized the gyroscope data with video data using the *pchip* method on MATLAB. We then computed the sum of the absolute gyroscope signal as overall dynamic body rotation (ODBR), analogous to ODBA,[65] to quantify motion of the body. Based on inspection of video data, we found the gyroscope was better able to separate behaviors, especially between walking and when birds were stationary but panting. Panting often occurs after flight to dissipate metabolic heat.[66,67] Takeoff and landing were determined manually from the gyroscope and video signals. We categorized data as from flight between takeoff and landing. We categorized data as from walking when ODBR was > 2 rad s^{-1} after landing. We categorized data as from standing when the bird had landed and was not within 2 s of walking. Outside of these categorizations, behavior was assigned as "non-specific" and data were not analyzed further.

Indoor landing data were processed similarly, except that we used acceleration rather than gyroscope data to categorize behavior, as the birds were only permitted to fly (ODBA > 20 m s^{-2}) between perches or to stand (ODBA < 4 m s^{-2}) on those perches.

All behavioral classifications were confirmed by viewing video data.

Eye tracking

We determined eye position by tracking 8 points around the margins of the pupil alongside stable features on the head (10–30 for outdoor trials, 4 for indoor landings) using DeepLabCut (ResNet-50).[10] Individual models were trained for each trial, as stable features varied between birds and were more conspicuous on some days than others. Files from DeepLabCut were then imported into MATLAB for processing.

We used markers on the front and back corners of the eye ring to determine both the orientation of the head in the camera view—to separate horizontal and vertical components of eye motion in an ego-centered reference frame—and the eye ring size—used to convert displacements in pixels to degrees of eye-in-head angle (see *Calibration of eye tracking system* section below). From both, we removed spikes when the camera bumped the wing or objects, filled these gaps via linear interpolation, and smoothed the data using a 1st-order Savitzky-Golay filter with a 3-second window.

For the other markers, we filtered out those with low confidence (thresholds ranged from 0.99–0.998) based on the output from DeepLabCut and expanded filtering by 100 ms on either side. Blinking obscures pupil markers. Thus, we determined the timing of blinks based on when any pupil marker had confidence below this threshold. We confirmed the accuracy of this method of detecting blinks by plotting non-filtered markers over the video data, frame-by-frame in MATLAB.

We rotated the remaining markers based on the orientation of the head such that ego-centered vertical movements occurred along the y-axis and horizontal along the x-axis. Then, we computed the position of the pupil relative to the stable head markers, in pixel units, by fitting an ellipse to the 8 pupil markers. This position was converted to displacement relative to the median position during flight. Displacement was converted to millimeters using the eye ring size in pixels (above) and the known size for each individual from separate scale photographs. Finally, the displacement in millimeters was converted to eye-in-head angle [based on[68]] using the estimated radius of rotation of the eye (distance between the pupil and the center of rotation of the eye) as

$$\theta = sin^{-1}\left(\frac{Displacement\ (mm)}{Radius\ of\ rotation\ (mm)}\right)$$

To detect saccades, we smoothed the eye-in-head angle using a 200 ms median filter.[69] Saccades were detected when horizontal or vertical velocities exceeded 40 deg s^{-1}, confirmed by manual inspection of the position data. Median filtered data was used only for saccade detection.

Pigeons blinked frequently while flying (2.2 ± 0.4 Hz), walking (2.1 ± 0.2 Hz), and standing (1.4 ± 0.3 Hz), interrupting eye tracking. Eye position also frequently changed during these interruptions. Given these features of the data, we found that typical smoothing algorithms for eye movement data either produced unnatural artifacts or aggressively trimmed the data because the window size was large relative to the length of each segment of data. As a form of low-pass filtering robust to blinks, we used least-squares linear fitting to extract the velocity of eye movements during each interblink interval (slope) and changes to eye position occurring during blinks (offset between successive fits).

Please cite this article in press as: Lapsansky et al., Pigeons make slow, divergent eye movements during flight and large, convergent eye movements when landing, Current Biology (2026), https://doi.org/10.1016/j.cub.2026.06.015

Calibration of eye tracking system

To calibrate the eye tracking system, we estimated eye's radius of rotation for each bird. We first modified the eye tracking system to record the eye from above (Figure S1A). We tracked four markers on the dorsal, ventral, rostral, and caudal margins of the pupil using DeepLabCut while birds made horizontal eye movements, which we elicited by gently rotating their head side to side.

In MATLAB, we computed the midpoint of the rostral–caudal marker pair for every frame. For each frame, we then constructed a ray that passed through this midpoint and was perpendicular to the line connecting the rostral and caudal markers. In the camera view, these rays radiate from the eye's center of rotation (Figure S1A). We estimated the intersection of these rays by minimizing the sum of squared distances to all such paths. The 2-D radius of rotation was then calculated as the mean distance between the rostral–caudal midpoint and the best-fit intersection point. Finally, we converted this 2-D distance to a 3-D estimate of radius of rotation by using the vertical-to-horizontal aspect ratio of the pupil, defined by the four markers, which indicates the perspective of the camera assuming a circular pupil.

We tested whether this process would provide a precise estimate of radius of rotation by repeating the procedure for a subset of birds on separate days under different light levels. We found the estimates were highly repeatable (Figure S1B). Between individuals, radii ranged from 3.7–5.5 mm and were correlated with both eye width (Figure S1C) and body mass (Figure S1D).

Binocular oculomotor response to translational optic flow

For head-fixed recordings of eye movement, a subset of pigeons (n = 5) were habituated to a head restraint system based on.[34] Pigeons were suspended in a flight posture from a custom-made "Abba"[70] and a small fan was used to generate feather vibration in the dark. The head was oriented as in flight, with an approximate eye-to-bill angle of 30 deg.[11] Stimuli were generated using PsychoPy (v. 2023.1.3) and presented on two 144 Hz LCD monitors (ASUS VG248QG, ASUSTeK Computer Inc., Taipei, Taiwan) set to sRGB color mode, resulting in gratings with a Michelson contrast of 0.99. The monitors were oriented perpendicular to the bird and positioned 30 cm away on either side, occupying approximately 83 deg horizontally and approximately 45 deg vertically on either side of the animal.

Stimuli consisted of square-wave gratings with a spatial frequency of 0.8 cyc deg^{-1} and horizontal speeds of 0, 0.62, 1.24, or 2.48 deg s^{-1}. Each recording session consisted of a set of trials in random order with each condition repeated five times. Each trial began with a static pattern for 1 second, followed by stationary gratings for 1 second, followed by 10 seconds of motion of those same gratings in either the temporo-nasal (TN) or naso-temporal (NT) direction. In trials where both gratings had non-zero speeds, both gratings moved at the same speed but in random directions (e.g., 1.24 deg s^{-1} TN to the right eye and 1.24 deg s^{-1} NT to the left eye, but not 2.48 deg s^{-1} TN to the right eye and 1.24 deg s^{-1} NT to the left eye).

To track the position of the pupil, two cameras (Prosilica GE 680, Allied Vision, Stadtroda, Germany) recording at 100 Hz (lossless AVI formatd) were positioned using tripods over the left and right sides of the bird to shoot over the top of each monitor (Figure 2A). We used a combination of thresholding and contour segmentation to fit an ellipse to each pupil and determine the orientation of that ellipse through time. Raw orientations were imported to MATLAB, wherein we synchronized these data with the timing of stimuli output by PsychoPy. For each trial, we normalized the orientation of the pupil relative to the median orientation during the 1 s blank period at the start of each trial.

Optic flow tracking

As with eye tracking videos, optic flow videos were recorded as H.264 video streams. H.264 compression is lossy and can introduce compression artifacts. We chose to maximize the recording rate of these videos (90 Hz) to reduce image displacement per sample and the impact of these compression artifacts. In contrast, recording videos in a lossless format (e.g., PNG stack) using this or other lightweight hardware is only possible at low frame rates (5–10 Hz).

Recordings were encoded to MKV video files using *ffmpeg* (FFV1 codec) before being converted to PNG image stacks. We then transformed image stacks to a rectilinear perspective using the *LensDistortion* tool in NukeX (Foundry, London, UK). This function used a 3rd-order polynomial division model of radial image distortion. Model parameters are estimated by minimizing the curvature of lines in the video that are known to be straight,[71,72] which we manually digitized (25 per video) using the *LensDistortion* tool. Straight features consisted mainly of lines on a quilter's ruler but also included the bars of the transport container or truck, in some cases. We then cropped the corners to remove highly stretched regions, resulting in rectangular, rectilinear image stacks for each video.

Optic flow cameras were oriented along the optical axis of the eye—60° lateral from straight forward (1). This orientation was confirmed by photographing the camera and mask from above after attaching the system to the bird and just before release. However, these cameras were sometimes tilted slightly downward or upward, and/or rolled about this 60° yaw orientation. To align each video (34 flights, 11 birds) to the same ego-centered reference frame as our eye movement data, we detected the tilt and roll of the horizon across 100 pseudo-random frames. These frames were randomly selected from the 3rd quartile of each flight, as birds tended to be highest above the trees during this period, improving horizon detection. The horizon was detected automatically via a covariance approach written in Python, which assumes that the horizon is the line that maximizes the variance between the sky and the ground and minimizes the within-region variance.[73] We found this method performed well for our optic flow videos. The median tilt and roll of the horizon, along with the fixed yaw of 60°, were used to position the rectilinear frames into the equirectangular projection.

Please cite this article in press as: Lapsansky et al., Pigeons make slow, divergent eye movements during flight and large, convergent eye movements when landing, Current Biology (2026), https://doi.org/10.1016/j.cub.2026.06.015

Rectilinear images were reprojected into equirectangular space (1800 by 900 pixels) using cubic interpolation based on their horizontal and vertical fields of view. These values were calculated from the sensor size, focal length of the lenses, and aspect ratio of the rectilinear images (image width / image height), as

$$hFOV = 2 * \text{atan}((sensor\ width) / (2 * focal\ length))$$

$$vFOV = 2 * \text{atan}\left(\tan\left(\frac{hFOV/2}{Aspect\ ratio}\right)\right)$$

We confirmed that these fields of view were accurate by separately recording a lens calibration tool (Arducam, Nanjing, CN). We wrote custom Python code to perform this transformation via parallel computing but confirmed that it matched the output from both the v360 plugin from *ffmpeg* and *SphericalTransform* tool in NukeX given the same input parameters.

Dense optical flow was calculated in Python using the Dense Inverse Search (DIS) algorithm with parameters set for highest precision.[74] This algorithm is both fast and has similar or higher accuracy than alternative methods at these settings.[75]

Python's optical flow methods assume a rectangular frame, but video data occupied a non-rectangular region dependent on the camera roll, pitch, and yaw, and the reprojection. To maximize the coverage area of optic flow data, we generated a set of overlapping rectangular patches within the bounds of the video data and computed the optical flow within each patch. We calculated optic flow (units: pixel frame^{-1}) for each pixel location as the median across overlapping patches after correcting the horizontal components for equirectangular distortion in proportion to cosine of latitude.[32]

In an equirectangular projection, horizontal distortion increases with latitude, in proportion to the cosine of latitude, as the image at the poles is stretched to occupy the same width as the equator. We corrected for this distortion by multiplying the horizontal component of the flow at each location by the cosine of the latitude (-90° to 90°) at that location.

To save memory, we reduced the spatial resolution of optic flow data from Python to one value per degree of visual angle (rather than one per pixel location) and imported to MATLAB for processing. In MATLAB, optic flow data were synchronized with inertial data (see above) and converted to units of deg frame^{-1}.

Head saccades generated fast, coherent optic flow across the entire frame. We categorized optic flow as generated by head saccades when the magnitude of optic flow, computed as the vector sum of median horizontal and vertical flow across the entire frame, exceeded its 1 second moving average by greater than two standard deviations. The accuracy of this threshold was confirmed by viewing the video data and prevented maneuvers around obstacles (e.g., trees) from being categorized as head saccades. Removing optic flow generated by head saccades left only discrete segments of optic flow produced by translation of the stable head.

To summarize the optic flow across trials, we computed the median flow (units: deg frame^{-1}) across a consistent set of 20° x 20° ROIs. First, we calculated the median horizontal and vertical flow within each region at each frame step. Then, we summed the optic flow occurring during each saccade-free segment of data for that region and divided by the duration of the segment (units: deg s^{-1}). Each of these values represents a sample of optic flow occurring in that region of the visual field for the period of time between head saccades.

QUANTIFICATION AND STATISTICAL ANALYSIS

Data analysis and plotting were conducted in R (version 4.4.1) with plots created using 'ggplot2' version 4.0.0. Details of statistical tests can be found in the main manuscript and figure captions. All data and code associated with this manuscript will be posted on Dryad upon acceptance. The number of individuals varied by experiment. Data in Figure 1 are from 16 trials from 5 birds, generating data for 27 min of flight, 29 min of standing, and 9 min of walking. Data in Figure 2 are from 34 trials from 11 birds. Data in Figure 3 are from 5 birds, wherein stimulus conditions were ordered randomly and recorded in series on a single session. Data for landings outdoors (Figures 4A and 4B) are based on 12 landings of 4 birds. We then confirmed convergence during landing by measuring eye position across 212 landings from an additional 3 individuals trained to fly perch to perch in the lab (panels C–H).